THE JOURNAL OF BIOLOGICAL CHEMISTRY VOL. 290, NO. 37, pp. 22841–22850, September 11, 2015
© 2015 by The American Society for Biochemistry and Molecular Biology, Inc. Published in the U.S.A.

The MLLE Domain of the Ubiquitin Ligase UBR5 Binds to Its Catalytic Domain to Regulate Substrate Binding*

Received for publication, June 12, 2015, and in revised form, July 17, 2015 Published, JBC Papers in Press, July 29, 2015, DOI 10.1074/jbc.M115.672246

Juliana Muñoz-Escobar[1], **Edna Matta-Camacho**[1,2], **Guennadi Kozlov, and Kalle Gehring**[3]

From the Department of Biochemistry, Groupe de Recherche Axé sur la Structure des Protéines, McGill University, Montréal, Québec H3G 0B1, Canada

Background: Paip2 and GW182 are translation effectors that interact with the E3 ubiquitin ligase UBR5.
Results: The MLLE domain of UBR5 interacts with GW182, recruits Paip2 for ubiquitination, and interacts with the catalytic HECT domain of UBR5.
Conclusion: The MLLE domain of UBR5 regulates inter- and intramolecular interactions in UBR5.
Significance: The MLLE/HECT interaction in UBR5 may regulate ubiquitin transfer catalyzed by the HECT domain.

E3 ubiquitin ligases catalyze the transfer of ubiquitin from an E2-conjugating enzyme to a substrate. UBR5, homologous to the E6AP C terminus (HECT)-type E3 ligase, mediates the ubiquitination of proteins involved in translation regulation, DNA damage response, and gluconeogenesis. In addition, UBR5 functions in a ligase-independent manner by prompting protein/protein interactions without ubiquitination of the binding partner. Despite recent functional studies, the mechanisms involved in substrate recognition and selective ubiquitination of its binding partners remain elusive. The C terminus of UBR5 harbors the HECT catalytic domain and an adjacent MLLE domain. MLLE domains mediate protein/protein interactions through the binding of a conserved peptide motif, termed PAM2. Here, we characterize the binding properties of the UBR5 MLLE domain to PAM2 peptides from Paip1 and GW182. The crystal structure with a Paip1 PAM2 peptide reveals the network of hydrophobic and ionic interactions that drive binding. In addition, we identify a novel interaction of the MLLE domain with the adjacent HECT domain mediated by a PAM2-like sequence. Our results confirm the role of the MLLE domain of UBR5 in substrate recruitment and suggest a potential role in regulating UBR5 ligase activity.

Ubiquitination is one of the most abundant post-translational modifications in eukaryotic cells. Catalyzed by the ubiquitin proteasome system, ubiquitination has two major roles as follows: regulation of protein degradation, essential for normal cellular function and for the removal of harmful, damaged, or misfolded proteins; and control of protein activity by regulating protein/protein interactions and subcellular localization (1, 2). The ubiquitin proteasome system targets proteins through the addition of one or more ubiquitin molecules to specific lysine residues or to the N terminus. This process is carried out by a complex cascade of reactions catalyzed by activating (E1), conjugating (E2), and ligating enzymes (2, 3). The E3 ubiquitin ligases mediate the specificity toward substrates and catalyze the final attachment of the 76-residue ubiquitin moiety to the target protein. E3 enzymes fall into two categories based on their catalytic mechanism: RING (Really Interesting New Gene) and U-box ligases promote ubiquitin transfer indirectly, whereas RBR (RING between RING) and HECT (homologous to E6-AP C terminus)-type ubiquitin ligases directly catalyze the transfer of ubiquitin to the substrate. In this latter category, the ubiquitin is transferred from the E2-conjugating enzyme to the substrate in a two-step reaction. In the first step, a catalytic cysteine in the E3 enzyme forms a thioester bond with the ubiquitin from the E2-ubiquitin intermediate. In the final step, ubiquitin is transferred from the thioester bond with the E3 to a lysine residue in the substrate (4).

Ubiquitin protein ligase E3 component N-recognin 5 (UBR5) also known as EDD (E3 isolated by differential display) is a mammalian ortholog of the HYD (hyperplastic discs) protein of *Drosophila melanogaster* (5, 6). UBR5 belongs to the HECT-type group of E3 ubiquitin ligases. Human UBR5 mediates ubiquitination of several proteins, including β-catenin, TopBP1, TERT, RORyt, Paip2, CDK9, ATMIN, among others, highlighting its role as an important effector in cell cycle progression and DNA damage response (7–15). UBR5 has also been suggested to be a tumor suppressor. Overexpressed or mutated UBR5 has been found in solid tumors, including ovarian, breast, hepatocellular, tongue, gastric, and melanoma (16–19). In addition, UBR5 exhibits E3-independent activity as a transcriptional cofactor for the progesterone receptor and serves as a binding partner for a diverse subset of proteins such as GW182, p53, CHK2, TFIIS, and DUBA (7, 8, 12, 20–23). Despite accumulating knowledge about UBR5 function, the biochemical roles and exact mechanisms of recognition and ubiquitination by UBR5 have yet to be determined.

* This work was supported by Canadian Institutes of Health Research Grant MOP-14219 (to K. G.) and an Natural Sciences and Engineering Research Council of Canada CREATE Training Program in Bionanomachines award (to J. M.). The authors declare that they have no conflict of interest with the contents of this article.

The atomic coordinates and structure factors (code 3NTW) have been deposited in the Protein Data Bank (http://wwpdb.org/).

[1] Both authors contributed equally to this work.
[2] Present address: Dept. of Biochemistry, The Rosalind and Morris Goodman Cancer Research Center, McGill University, Montréal, Québec H3G 1Y6, Canada.
[3] To whom correspondence should be addressed: Dept. of Biochemistry, McGill University, 3649 Promenade Sir William Osler, Montréal, Québec H3G 0B1, Canada. Tel. 514- 398-7287; E-mail: kalle.gehring@mcgill.ca.

This is an open access article under the CC BY license.

UBR5 is a large 309-kDa protein and consists of a N-terminal UBA domain followed by two nuclear localization signals, a zinc finger-like UBR-box, an MLLE domain homologous to the C-terminal domain of poly(A)-binding protein (PABP), and a HECT[4] domain at its C terminus (Fig. 1*A*) (24–26). Remarkably, only two proteins in eukaryotic cells contain an MLLE domain, PABP and UBR5. In PABP, MLLE is a protein/protein interaction domain that recognizes effectors of translation initiation that display a conserved peptide motif, PAM2 (PABP-interacting motif 2) (25). The term MLLE comes from a signature motif MLLEKITG in the domain and the abbreviation of Mademoiselle in French. Solution and crystal structures of the MLLE domains from human UBR5 and various PABPs have shown that the domains consist of a bundle of 4 or 5 α-helices (25, 27). The PAM2 motif was initially identified in the following three proteins associated with mRNA translation and protein synthesis: Paip1 (PABP-interacting protein 1), Paip2, and eukaryotic release factor 3 (28). A bioinformatic survey highlighted the existence of many other PAM2-containing proteins, which include ataxin-2, Tob1/2, USP10, dNF-X1, TPRD/TTC3, and dMAP 205 kDa (29). The NMR solution and crystal structures of the MLLE domain from human PABP in complex with PAM2 peptides revealed that peptides bind to the most conserved helices α2, α3, and α5 of MLLE (30–32). Recently, GW182 was shown to bind to the PABP MLLE surface largely overlapping with the PAM2-binding site (33, 34).

Accumulating evidence supports the model in which competition between UBR5 and PABP for shared binding partners is linked to translation and gene expression regulation. This has been demonstrated for UBR5-mediated proteasomal degradation of Paip2 upon PABP depletion (14) and for the recruitment of GW182 and Tob1/2 by UBR5 to Argonaute-miRNA complexes during gene silencing (23).

The MLLE domain of UBR5 was first shown to bind to a fragment of Paip1 by GST-pulldown assays (27). The peptide binding properties of the UBR5 MLLE domain were later characterized by our laboratory using NMR chemical shift mapping and isothermal titration calorimetry (32). Despite previous studies, there is no atomic structure for UBR5 MLLE bound to a PAM2 peptide. Moreover, the binding of GW182 to UBR5 in miRNA silencing has not been characterized.

A number of substrates for ubiquitination by UBR5 have been described in the last few years. In numerous cases, the C-terminal fragment of UBR5 that includes the MLLE and HECT domains mediates binding. These observations suggest a role of the MLLE domain in the substrate selectivity of UBR5. For instance, Paip2 is targeted for proteasomal degradation by UBR5. However, it is unclear whether this interaction is mediated directly by the MLLE domain. A better understanding of PAM2 recognition by UBR5 should help in the identification of novel physiological partners and provide insight into its ability to regulate ubiquitin and E3-independent activity.

In this study, we determined the crystal structure of the MLLE domain of UBR5 in complex with the PAM2 peptide from Paip1. The structure explains the overlapping binding specificity of the MLLE domains from UBR5 and PABP. We reveal a novel intramolecular interaction involving the MLLE domain and the HECT domain of UBR5. This interaction is mapped to the N-terminal lobe in the HECT domain and is mediated by a PAM2-like sequence. Our results suggest a regulatory role of the MLLE domain in the catalytic activity of UBR5 beyond binding of PAM2-containing substrates.

Experimental Procedures

Protein Expression, Purification, and Peptide Synthesis—Human Paip2 protein and the MLLE, HECT, and MLLE-HECT domains of rat UBR5 were cloned into BamHI and XhoI restriction sites of the pGEX-6P-1 vector (Amersham Biosciences), and the construct was transformed into the *Escherichia coli* expression host BL21 Gold Magic (DE3) (Stratagene). The proteins were expressed and purified by affinity chromatography to yield a GST-fused domain or an isolated domain with a five-residue (Gly-Pro-Leu-Gly-Ser) N-terminal extension. Prior to crystallization, the MLLE protein was additionally purified using size-exclusion chromatography in gel filtration buffer (50 mM Tris, 100 mM NaCl (pH 7.5)). The final yield of purified protein was ~7 mg/liter of Luria broth culture media.

A plasmid coding for the full-length human UBR5 was kindly donated by Dr. Darren N. Saunders (Garvan Institute of Medical Research), and the protein was expressed in HEK293 cells as a His tag fusion protein.

The Paip1(123–144), Paip2(106–127), and GW182(1380–1401) peptides were synthesized by Fmoc solid-phase peptide synthesis and purified by reverse-phase chromatography on a C18 column (Vydac, Hesperia, CA). The composition and purity of the peptides were verified by electrospray ionization mass spectroscopy. The HECT peptide and its F2505A mutant were expressed as GST-fused proteins in *E. coli*, purified with affinity chromatography, and cleaved with PreScission protease leaving a five-residue (Gly-Pro-Leu-Gly-Ser) N-terminal extension. Peptides were further purified by reverse-phase chromatography. Western blot analyses were done using anti-UBR5 and anti-Paip2 antibodies (Sigma).

Isothermal Titration Calorimetry Measurements—Experiments were carried out on a MicroCal iTC200 titration calorimeter in 50 mM Tris-HCl buffer (pH 7.6) and 150 mM NaCl at 20 °C. The reaction cell contained 200 μl of 0.1 mM HECT-N lobe and was titrated with 19 injections of 2 μl of 1.0 mM MLLE domain. The binding isotherm was fit with a binding model employing a single set of independent sites to determine the thermodynamic binding constants and stoichiometry.

Crystallization—Crystallization conditions for the UBR5 MLLE·Paip1(123–144) complex were identified utilizing hanging drop vapor diffusion with the JCSG+ crystallization suite (Qiagen). The best crystals were obtained by equilibrating a 1.0-μl drop of MLLE-Paip1(123–144) mixture in a 1:2 ratio (10 mg/ml) in 50 mM Tris-HCl (pH 7.5), 0.1 M NaCl, mixed with 1.0 μl of reservoir solution containing 1.0 M ammonium sulfate, 0.2 M lithium sulfate, 10% glycerol, and 0.1 M Tris-HCl (pH 8.5). Crystals grew in 3–10 days at 20 °C. The crystals contain two MLLE and two peptide molecules in the asymmetric unit corresponding to V_m = 2.89 Å^3 Da^{-1} and a solvent content of

[4] The abbreviations used are: HECT, homologous to the E6AP C terminus; PABP, poly(A)-binding protein; r.m.s.d., root mean square deviation.

57.4%. Residue numbers used here and in the PDB deposition are 14 less than in UniProt entry Q62671.

Structure Solution and Refinement—Diffraction data from a single crystal of the MLLE·peptide complex were collected on an ADSC Quantum-210 CCD detector (Area Detector Systems Corp.) at beamline A1 at the Cornell High Energy Synchrotron Source (CHESS) (Table 1). Data processing and scaling were performed with HKL2000 (11). The structure of UBR5 MLLE/Paip1 was determined by molecular replacement with Phaser (35), using the coordinates of MLLE from human UBR5 (PDB entry 1I2T). The initial model obtained from Phaser was completed and adjusted with the program Xfit (36) and was improved by several cycles of refinement, using the program REFMAC 5.2 (37) and model refitting. At the latest stage of refinement, we also applied the translation-libration-screw (TLS) option (38). The final model has good stereochemistry according to the program PROCHECK (39) and WHAT IF (40). The refinement statistics are given in Table 1. The coordinates and structure factors have been deposited in the RCSB Protein Data Bank (accession number 3NTW).

NMR Spectroscopy—NMR assignments of the MLLE domain of rat UBR5 were described earlier (32). All NMR experiments were recorded at 298 K. NMR titrations were carried out by adding either unlabeled protein or peptide into 0.15 mM samples of the ^{15}N-labeled MLLE domain and monitored by ^{15}N-^{1}H heteronuclear single quantum correlation spectra. NMR spectra were processed using NMRPipe (41) and analyzed with XEASY (42).

Results

GW182 Interacts with the UBR5 MLLE Domain—Human GW182, a core component of the miRNA-induced silencing complex, interacts with PABP via its MLLE domain, and this interaction is required for miRNA-mediated deadenylation (33, 34). In a similar fashion, UBR5 was recently suggested to be a key component of the miRNA-silencing pathway with the MLLE domain being essential for its silencing function (23). UBR5 regulated miRNA-mediated gene silencing in an E3 ligase-independent manner by targeting the GW182 family of Argonaute·miRNA complexes. In this study, UBR5 recruited the translation effectors GW182 and Tob1/2 without prompting their proteasomal degradation. Previous studies have characterized the binding properties of several effectors of translation initiation that interact with the PABP MLLE domain through PAM2 motifs. To understand the ability of UBR5 to bind GW182, we performed a titration of the ^{15}N-labeled UBR5 MLLE domain with GW182(1380–1401). Addition of the peptide produced large chemical shift changes in a number of amides, indicating specific binding (Fig. 1*B*). The titration resulted in fast-intermediate exchange that suggests high micromolar binding affinity. A fit of the chemical shift changes measured a K_d of 175 ± 35 μM. Although significantly weaker than the interaction with the PABP MLLE domain (6 μM), the chemical shift changes upon GW182 binding are similar to those seen upon binding the PAM2 peptide from Paip1 (Fig. 1*C*). The largest chemical shift changes upon GW182 peptide binding were leucine, threonine, lysine, glycine, and alanine residues in helices α2, α3, and the C terminus of helix α5 (Fig. 1*D*). This confirms that GW182 binds the UBR5 MLLE domain through its PAM2 motif as seen in other PAM2-containing proteins.

Structure of UBR5 MLLE Bound to a PAM2 Peptide—To further understand the binding specificity of the MLLE domain from UBR5, we attempted to crystallize the domain in complex with the GW182 peptide. However, no crystals were obtained during crystallization trials. Alternatively, we were able to obtain diffracting crystals for MLLE in complex with the Paip1 peptide. This peptide showed the highest affinity (K_d of 3.4 μM) among those tested in previous isothermal titration calorimetry studies (32). The asymmetric unit contains two copies of the MLLE·peptide complex, which are very similar with an r.m.s.d. of 0.24 Å over 58 Cα atoms. The electron density was missing for three and six residues at the N and C termini of the Paip1 peptide suggesting they are disordered (Table 1).

The structure of the peptide-bound UBR5 MLLE shows a helical bundle with four α-helices folding into a right-handed superhelix. When compared with the structure of the unliganded domain from human UBR5 (27), both structures are very similar, displaying an r.m.s.d. of 0.72 Å over residues Gln-2381–Ala-2437. The only significant difference can be seen in the N-terminal helix, which slightly bends toward the peptide in the complex structure (Fig. 2*A*). As the structure of the MLLE domain from PABP contains the additional α-helix at the N terminus (25), the helices in the domain from UBR5 are numbered from α2 to α5 for easier comparison. In the complex, the Paip1 peptide adopts an extended conformation except for a β-turn at residues Ser-129–Ala-132 that allows it to wrap around the highly conserved helix α3.

Hydrophobic interactions make major contributions to peptide binding to MLLE domains (33). The side chain of Paip1 Phe-135 interacts with Cα of Gly-2384, the methyl group of Thr-2403, and stacks with the side chain of Tyr-2388 in a classical "fishbone" stacking arrangement (Fig. 2*B*). Next to it, the side chain of Pro-137 packs against the aromatic ring of Tyr-2388. The side chain of Leu-128 inserts into a hydrophobic pocket formed by the side chains of Met-2405, Leu-2406, Leu-2409, Ala-2431, Leu-2434, and the aliphatic part of Glu-2430 (Fig. 2*C*). An additional hydrophobic interaction involves Ala-132 of Paip1, which is invariant in PAM2 sequences. The methyl group of Ala-132 packs against Cα of Met-2405, carbonyl of Gly-2404, and the Cγ of Glu-2408 (Fig. 2*C*).

The peptide binding is reinforced by ionic interactions with the UBR5 MLLE domain. The carbonyls of Val-130 and Ala-132 form hydrogen bonds with the side chain of Lys-2401 (Fig. 2*C*). The amide of Phe-135 forms a hydrogen bond with the carbonyl and the side chain of Ser-2400 (Fig. 2*B*), which also makes hydrogen bonds with the carbonyl of Phe-135. The carbonyl of Tyr-136 makes a hydrogen bond with the side chain of Gln-2381. The side chain of Glu-2385 makes a salt bridge with side chain and amide of Ser-138 (Fig. 2*B*). The side chain of Ser-129 makes a salt bridge with the side chain of Glu-2408. Carbonyl of this serine makes an intramolecular hydrogen bond with the amide of Ala-132, which stabilizes the bound conformation of the peptide (Fig. 2*C*).

UBR5 Binds Paip2—Conservation in the binding properties of the MLLE domains from PABP and UBR5 suggests that the

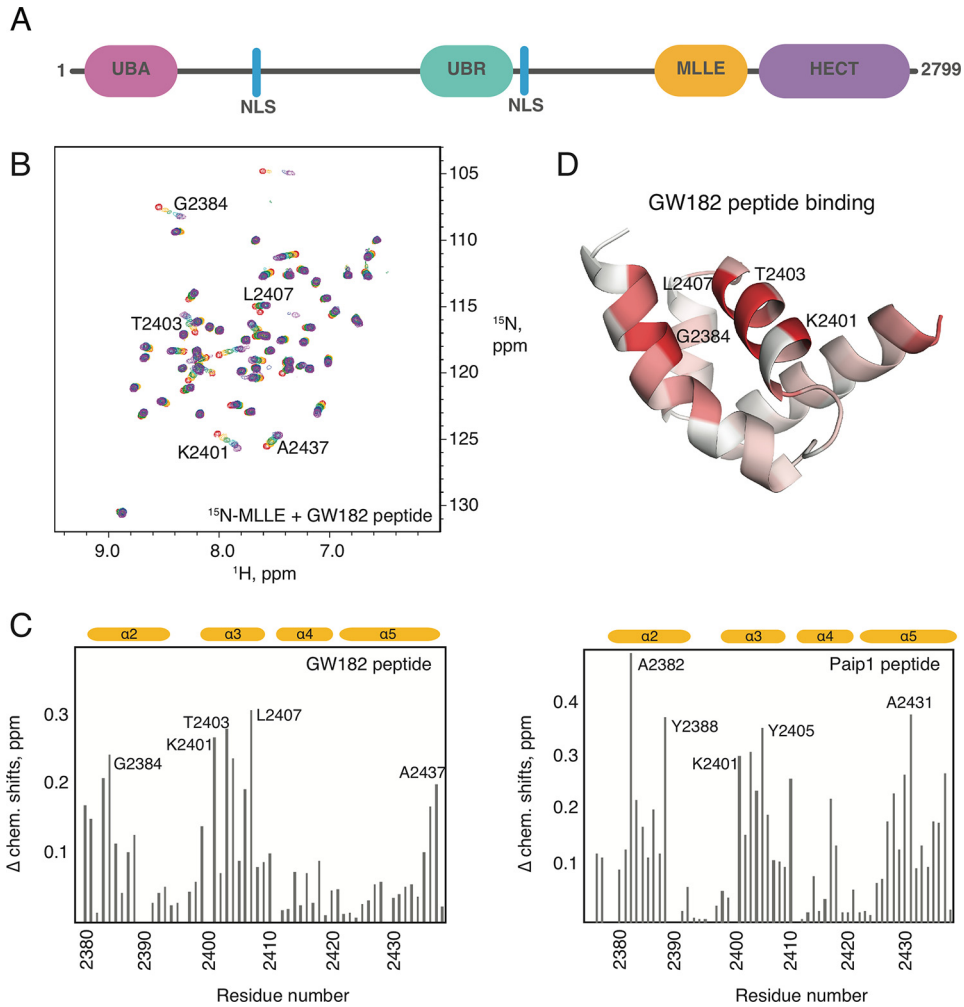

FIGURE 1. **GW182 PAM2-like region interacts with UBR5 MLLE.** *A,* schematic diagram of the structural domains of UBR5. The catalytic HECT domain is at the C terminus. UBR5 also contains two nuclear localization signals (*NLS*) and three protein/protein interaction domains as follows: a ubiquitin-associated domain at its N terminus, a zinc finger-like UBR domain near the middle of the protein, and a domain homologous to the C-terminal domain of poly(A)-binding protein called the MLLE domain that is adjacent to the HECT domain. *B,* ^{15}N-^{1}H NMR correlation spectra of the ^{15}N-labeled UBR5 MLLE domain titrated with increasing amounts of the GW182(1380–1401) peptide, color-coded from *red* to *purple*. *C,* comparison of the chemical shift changes in the ^{15}N-labeled UBR5 MLLE domain upon addition of the GW182 peptide (*left*) and Paip1 peptide (*right*). Shifts are calculated as a weighted average in ppm as $(\Delta H^2 + (\Delta N/5)^2)^{1/2}$. *D,* mapping of the NMR chemical shift changes onto a schematic representation of the unliganded MLLE domain (PDB entry 1I2T) upon binding of GW182 (*white,* no change; *red,* maximum change). Helices α2, α3, and α5 of UBR5 MLLE are involved in peptide binding.

E3 ubiquitin ligase activity of UBR5 may play a role in translation. For instance, UBR5 targets the translation inhibitor Paip2 for ubiquitination and proteasomal degradation when PABP is depleted (14). To confirm this is due to a direct interaction, we tested binding of Paip2 to full-length UBR5 and the UBR5 MLLE-HECT fragment (Fig. 1*A*). We performed a series of pulldown assays using GST-fused full-length Paip2 as bait for binding to the full-length UBR5 (Fig. 3*A*) and GST-MLLE or GST-MLLE-HECT fragments of UBR5 as bait for Paip2 binding (Fig. 3*B*). In all cases binding of Paip2 to either the full-length UBR5 or the MLLE-containing fragments was observed. The presence of a phenylalanine residue in PAM2 motifs is conserved throughout PAM2-containing proteins and is required for their interactions with MLLE domains (30). We tested whether the Phe-118 of Paip2 was required for the interaction with UBR5 in our binding assays. The Paip2 F118A mutation abrogated binding to both full-length UBR5 and its MLLE domain confirming that the interaction was direct and specific to the MLLE domain of UBR5 (Fig. 3, *A* and *B*).

MLLE Interacts with the HECT Domain of UBR5—The ability of UBR5 to regulate its activity throughout the many pathways it is involved in remains elusive. In E3 ligases, often sequences or domains located in proximity to the HECT domain are involved in intra- and/or intermolecular interactions that modulate the catalytic activity (4, 43–45). The MLLE domain in UBR5 is located at the N-terminal side of the catalytic HECT domain with an ~50-residue separation. Thus, we asked whether the MLLE domain might interact with the HECT domain. To test this, we performed an NMR titration of ^{15}N-labeled MLLE (Fig. 4*A*) with the unlabeled GST-fused HECT domain (residues 2520–2799). Stepwise addition of the GST-HECT domain resulted in severe line broadening and the loss of most of the peaks in the NMR spectrum (Fig. 4*B*) suggesting formation of a high molecular weight complex. As controls, titrations of MLLE with GST, with the UBA domain (residues 180–230), or with the UBR box (residues 1177–1244) of UBR5 showed no spectral changes, indicating no binding (data not shown). An additional control with the MLLE domain of PABP

TABLE 1
Data collection and refinement statistics

	UBR5 MLLE-Paip1(123–144)
Data collection	
Space group	$P6_422$
Cell dimensions	
a, *b*, *c* (Å)	95.79, 95.79, 82.94
Resolution (Å)	50–2.60 (2.69–2.60)[a]
R_{sym}	0.054 (0.343)
$I/\sigma I$	24.2 (6.6)
Completeness (%)	99.9 (100.0)
Redundancy	10.1 (8.9)
Refinement	
Resolution (Å)	41.5–2.60
No. of reflections	6999
R_{work}/R_{free}	0.227/0.289
No. of atoms	1110
MLLE	902
Peptide	200
Water	8
B-Factors	
MLLE	16.4
Peptide	24.0
Water	48.3
R.m.s deviations	
Bond lengths (Å)	0.018
Bond angles (°)	2.06
Ramachandran statistics (%)	
Most favored regions	93.4
Additional allowed regions	6.6
WHAT IF structure *Z*-scores[b]	
1st generation packing quality	0.9
2nd generation packing quality	1.3
Ramachandran plot appearance	0.5
χ-1/χ-2 rotamer normality	−1.7
Backbone conformation	1.4
WHAT IF RMS Z-scores[c]	
Bond lengths	0.796
Bond angles	0.954
Ω angle restraints	1.007
Side chain planarity	0.709
Improper dihedral distribution	1.075
B-Factor distribution	0.509
Inside/outside distribution	1.008

[a] Highest resolution shell is shown in parentheses.
[b] Values were calculated on secondary structure elements. A *Z*-score is defined as the deviation from the average value for this indicator observed in a database of high resolution crystal structures, expressed in units of the standard deviation of this database-derived average. Typically, *Z*-scores below a value of −3 are considered poor; those below −4 are considered bad.
[c] Values were calculated on all residues.

showed that HECT binding was limited to the MLLE domain of UBR5 (data not shown). Together, these data demonstrate that the MLLE domain of UBR5 specifically binds to its HECT domain.

The HECT domain of E3 ligases consists of a bilobal structure with a C-terminal lobe containing the catalytic cysteine residue and an N-terminal lobe that binds the E2 enzyme. The lobes are linked by a flexible region, which presumably facilitates proper positioning of the catalytic cysteine toward the ubiquitin-E2 thioester bond (4). Our next question involved the characterization of the MLLE/HECT interaction and, in particular, how the N- and C-terminal lobes of the HECT domain were involved. We expressed and purified independently the N-lobe (residues 2520–2662) and C-lobe (residues 2687–2799) of UBR5. Addition of the C-lobe fragment to ^{15}N-labeled MLLE produced no spectral changes indicating no binding (Fig. 4*C*). Conversely, the addition of the N-lobe fragment to ^{15}N-labeled MLLE produced strong line broadening similar to that observed with the HECT domain (Fig. 4*D*). Next, we tested whether the MLLE/N-lobe interaction required the peptide-binding surface of the MLLE domain by adding a PAM2 peptide to the complex of MLLE and N-lobe domains. If the MLLE/N-lobe interaction was dependent on the PAM2-recognizing surface of MLLE, then the peptide would compete with the N-lobe for MLLE, and the NMR signals would reappear, which is what we observed. Addition of a peptide corresponding to residues 106–127 of Paip2 resulted in the reappearance of signals for MLLE at the positions consistent with MLLE binding the PAM2 peptide (Fig. 4*E*). Isothermal titration calorimetry measurements of the MLLE/N-lobe interaction measured a K_d of 50 ± 2.0 μM (Fig. 4*F*). These results show that the MLLE domain from UBR5 interacts with the HECT domain in a PAM2-dependent manner.

N-terminal Lobe of the HECT Domain Contains a PAM2-like Sequence—The alignment of the PAM2 sequences from the proteins known to bind PABP and/or UBR5 to the HECT domain revealed the presence of a sequence in the N-terminal lobe with features of a PAM2 motif (Fig. 5*A*). The Phe-2505 in the N-lobe of UBR5 can be aligned with the conserved phenylalanine of other PAM2-containing proteins. Conserved asparagine and alanine residues are also present in the N-lobe. We designed a peptide bearing the HECT PAM2-like sequence (residues 2499–2517) and performed two-dimensional NMR titrations using ^{15}N-labeled MLLE from UBR5. Titration of the ^{15}N-labeled MLLE with the HECT peptide produced large amide chemical shift changes in fast-intermediate exchange (Fig. 5*B*). The largest chemical shift changes occur in helices α2, α3, and α5 (Fig. 5*C*). The changes upon HECT peptide binding are similar to those seen upon binding of GW182 and Paip1 (Fig. 1*C*). A fit of the chemical shift changes measured a K_d of 850 ± 55 μM. The weak binding affinity of the peptide suggests that additional intramolecular contacts between HECT N-lobe and MLLE stabilize the association between the intact protein domains. As a control, we tested a second peptide with a mutation in Phe-2505. Upon addition of the F2505A peptide, there were almost no changes in the spectrum, indicating abrogation of the binding between MLLE and the mutant peptide (Fig. 5*D*).

Discussion

The specificity of the ubiquitination process relies on the E3 ubiquitin ligases and their ability to directly interact with substrates. Over 600 different E3s have been identified in the human genome, and 28 belong to the HECT-type E3 family. In all cases, the HECT domain is located at the C terminus of the protein, and the substrate binding is mediated by various domains located N-terminal to the HECT domain (4). The activity by HECT E3s can be regulated at two levels. In the first level, substrate binding is mediated through protein/protein interactions by domains/motifs located N-terminal to the HECT domain. Some HECT proteins also interact with regulatory/auxiliary proteins that facilitate or interfere with substrate binding (46–48). In the second level, regulation occurs through intra- and/or intermolecular interactions that inhibit ubiquitin-thioester formation or E2 binding (43–45, 49). Despite accumulating functional knowledge about the regulatory mechanisms that govern E3 ligases, our structural understanding of the inter- and intramolecular interactions that modulate the catalytic activity of HECT-type enzymes has lagged. The

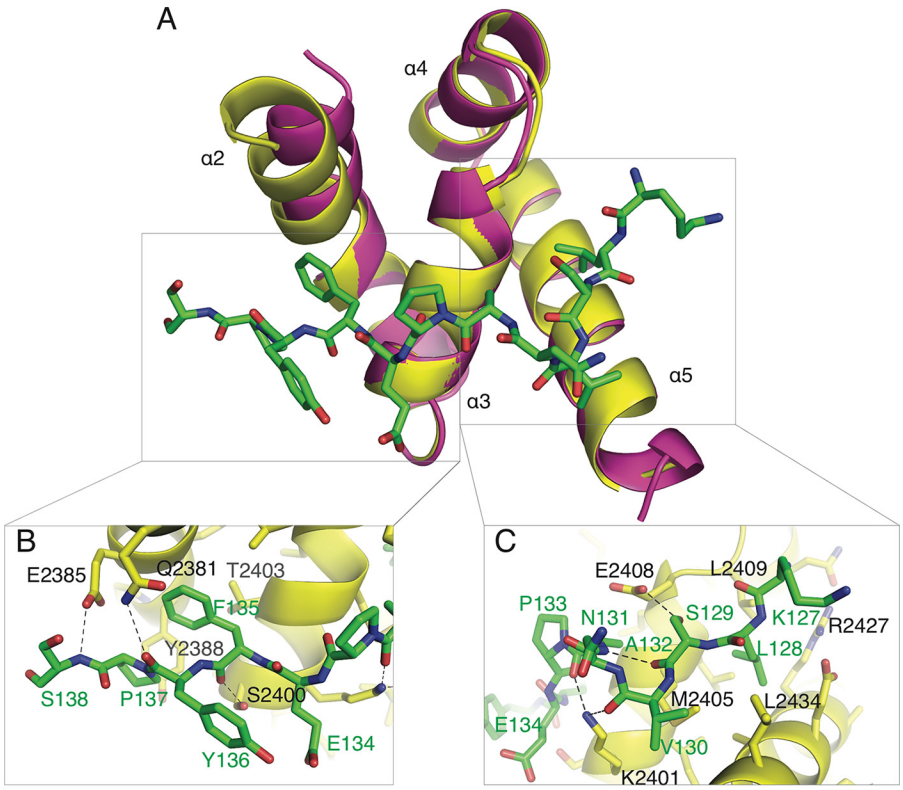

FIGURE 2. **Crystal structure of the UBR5 MLLE·Paip1 peptide complex.** *A,* UBR5 MLLE domain undergoes minor conformational changes upon binding the PAM2 peptide from Paip1. *Ribbon* representation of overlaid structures of the liganded (*yellow*) and unliganded (*magenta*; PDB entry 1I2T) MLLE domain from UBR5 is shown. The Paip1 peptide residues are shown as *green sticks*. *B,* close-up of the side chains of Gln-2381 and Glu-2385 of MLLE shows intermolecular hydrogen bonds with carbonyl of Pro-137 and amide of Ser-138 of Paip1. The aromatic ring of Paip1 Phe-135 stacks with the side chain of Tyr-2388. *C,* side chain of Lys-2401 of MLLE forms intermolecular hydrogen bonds with carbonyls of Val-130 and Ala-132 of Paip1. The hydrophobic side chain of Leu-128 plays a key role binding the MLLE domain.

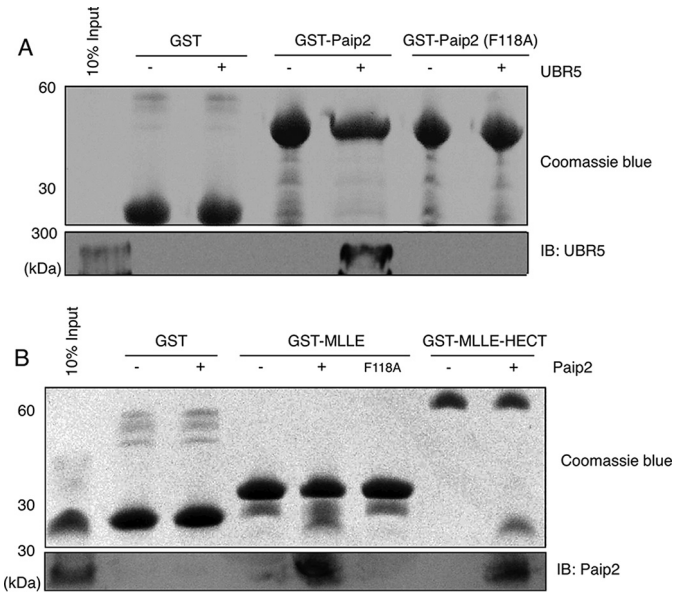

FIGURE 3. **Binding of Paip2 to UBR5.** *A,* binding of wild-type GST-Paip2 to full-length human UBR5. A mutation of a key phenylalanine residue in Paip2 prevents binding. *B,* binding of wild-type Paip2 or its F118A mutant to GST-MLLE or GST-MLLE-HECT fragments of UBR5. *IB*, immunoblot.

HECT-type ligases in the Nedd4 family are the most studied to date. In SMURF2, the C2 domain interacts with the HECT domain rendering the full-length protein inactive. The N-terminal lobe of the HECT domain interacts with the C2 domain and with ubiquitin. Both interacting surfaces overlap, affecting transthiolation and noncovalent binding of ubiquitin to the N-lobe (44). In the case of Itch, the autoinhibitory mechanism involves an intramolecular interaction between the WW domains and the HECT domain. Phosphorylation of the PRR regions of Itch causes a conformational change that weakens the WW/HECT interaction increasing its catalytic activity (43). A similar regulatory mechanism is seen in the non-Nedd4 HECT-type ligase HUWE1. An N-terminal helical element was shown to affect the catalytic activity of the HECT domain in HUWE1. In the absence of this N-terminal helix, the isolated HECT domain gained activity relative to the helix-extended counterpart; the authors hypothesize that this could be due to an increase in the inner flexibility of the HECT domain that allows the enzyme to acquire a favorable orientation for ubiquitin transfer or product release (49).

In the case of UBR5, we have identified an intramolecular interaction between the HECT domain and the adjacent MLLE domain. This interaction has the potential to regulate the catalytic activity of HECT in a manner similar to that seen in other E3 ligases. We measured the affinity of the interaction between the isolated domains to be 50 μM, which is relatively strong considering that, in the intact UBR5 protein, the two domains are separated by only 50 amino acids (Fig. 3*A*). Previous phosphoproteomic studies have reported UBR5 to be heavily phosphorylated (50). It is possible that specific phosphorylation sites in the protein lead to conformational changes that regulate

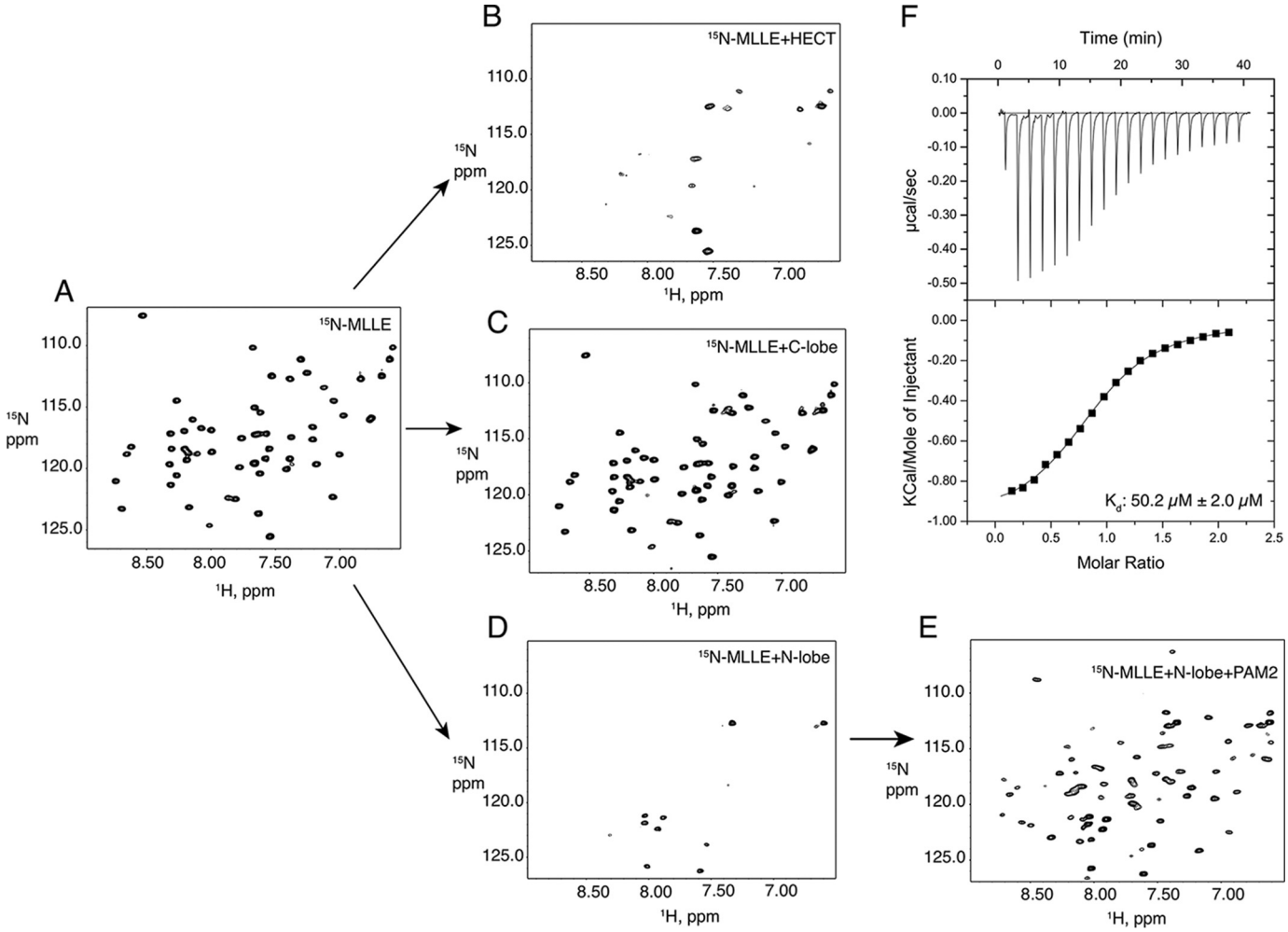

FIGURE 4. **UBR5 MLLE domain interacts with the HECT domain.** ^{1}H-^{15}N correlation NMR spectra of the ^{15}N-MLLE domain show that the isolated domain forms a higher molecular weight complex in the presence of the HECT domain. *A,* NMR spectrum of 0.15 mM ^{15}N-MLLE alone. *B,* NMR spectrum upon addition of 0.4 mM HECT domain. The fast transverse relaxation of magnetization due to the ^{15}N-MLLE/HECT interaction leads to loss of most of the MLLE NMR signals. *C,* NMR spectrum after addition of 0.5 mM C-lobe domain shows no interaction. *D,* NMR spectrum after addition of 0.5 mM N-lobe shows an interaction. *E,* addition of 1.1 mM Paip2(106–127) peptide leads to reappearance of the MLLE signals due to displacement of the N-lobe and the lower molecular weight of the MLLE·Paip2 peptide complex. *F,* isothermal titration calorimetry experiment for the binding of the N-terminal lobe of the HECT domain to the MLLE domain. The *upper curve* shows the baseline-corrected thermograph, and the *lower graph* shows the integrated areas of the heat of binding along with a fit, from which the stoichiometry (*N*) is 0.900 ± 0.007 sites, the molar association constant (*K*) is (1.99 ± 0.08) × 10^{4} M^{-1}, enthalpy (ΔH) is −1003 ± 11 cal/mol, and entropy (ΔS) is 16.3 cal/mol/degree.

ubiquitin activity. The MLLE/HECT interaction might regulate HECT domain activity by preventing proper E2 binding or positioning of the C-lobe to receive the ubiquitin. In parallel, the MLLE domain also acts as a substrate-binding domain so that substrate binding might be correlated with activation of ligase activity.

UBR5 plays an essential role in cellular processes such as DNA damage response, translation initiation, and cell cycle progression. However, the mechanistic details of how UBR5 interacts with substrates are poorly understood. To date, the only PAM2-containing protein identified as a substrate for ubiquitination and proteasomal degradation by UBR5 is Paip2. Yoshida *et al.* (14) proposed a homeostatic mechanism where PABP and UBR5 compete for binding to Paip2, an inhibitor of PABP function. A decrease in PABP levels augments the concentration of Paip2 that is available to interact with UBR5, leading to Paip2 proteasomal degradation. As Paip2 levels decrease, the relative amount of PABP increases, and the overall activity of PABP is restored in a positive feedback. In contrast, UBR5 plays an essential role in microRNA-mediated gene silencing independent of its ubiquitin ligase activity (23). To date, there are two suggested roles of the MLLE domain in miRNA silencing. First, GW182 proteins recruit UBR5 into Ago·miRNA complexes through its MLLE domain. Second, UBR5 MLLE interacts with PAM2-containing proteins in a similar fashion to PABP thus sharing binding partners such as Paip1/2 and Tob1/2. Through protein interactions with these proteins, the extended protein network includes different deadenylase complexes, all of which play key roles in regulating translation and mRNA stability. In this study, we characterized the binding of the UBR5 MLLE domain to the GW182 PAM2 peptide and solved the crystal structure of the MLLE·Paip1 complex. Comparison of the MLLE domains of UBR5 and PABP shows that the major intermolecular interactions that mediate peptide binding are preserved in both proteins. However, in general, the affinity of the UBR5 MLLE domain for PAM2 peptides is lower

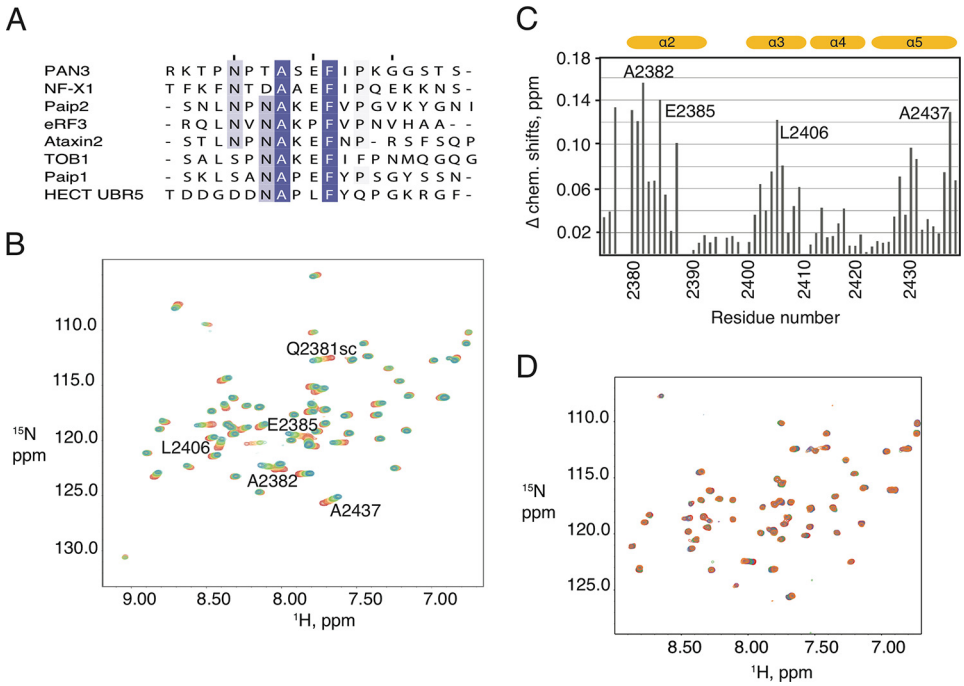

FIGURE 5. **UBR5 MLLE domain recognizes a PAM2-like peptide from the UBR5 HECT domain.** *A,* sequence alignment of known PAM2 motifs and a PAM2-like sequence in the N-terminal lobe of the HECT domain. *B,* ^{1}H-^{15}N correlation NMR spectra ^{15}N-MLLE domain of UBR5 titrated with increasing concentrations of the HECT peptide. *Red* is the spectrum of ^{15}N-MLLE alone, and *blue* is the spectrum with the highest concentration of peptide. *C,* chemical shift changes in the ^{15}N-labeled UBR5 MLLE domain upon addition of HECT peptide. The largest chemical shift changes were by Arg-2380, Ala-2382, Glu-2385, and Tyr-2388 positioned in helix α2, Leu-2406 in helix α3, and Ala-2437 in helix α5. *D,* NMR spectra titrated with increasing concentrations of the mutant HECT peptide (F2505A) show no significant changes.

than that of the PABP MLLE domain. The complex with the GW182 peptide is no exception. The GW182 PAM2 peptide binds to UBR5 MLLE with ~30-fold lower affinity than to the PABP MLLE domain (33). This likely reflects the unique C-terminal sequence of the GW182 PAM2 motif, which contains a tryptophan residue that inserts between the helices α2 and α3 of PABP MLLE (32, 34). The biological significance of the wide range of PAM2 affinities measured *in vitro* is unclear. It would be interesting to investigate the functional significance of the differences in affinity for GW182 in the Ago·miRNA complex formation.

The binding of the PAM2 peptides to UBR5 shows surprising contrasts in function. PAM2 motifs from GW182 and Paip2 have the ability to bind the MLLE domains from both UBR5 and PABP, but with a higher affinity for the latter. However, the proteins interact with UBR5 for different purposes. Paip2's fate is to be targeted for proteasomal degradation, whereas GW182 promotes gene silencing. In contrast, the interaction of the PAM2 peptide from the HECT domain of UBR5 suggests a role in regulating UBR5 activity. Despite the fact that all of these interactions involve recognition of PAM2-like sequences, each of them seems to have a unique effect in the response of UBR5. It remains to be discovered whether the differences in affinity among PAM2 proteins are essential in determining the role of UBR5 or whether other events are key in controlling the different activities of UBR5.

In conclusion, we have characterized the PAM2 peptide binding to the MLLE domain of UBR5 by x-ray crystallography and NMR spectroscopy. Future functional and structural studies are required to address the role of the newly discovered MLLE/HECT interaction in the E3 ligase activity of UBR5.

Author Contributions—K. G. coordinated the study. J. M. E., E. M. C., G. K., and K. G. wrote the paper. G. K. designed, performed, and analyzed the experiment shown in Figs. 1 and 2. E. M. C. designed, performed, and analyzed experiments seen in Figs. 3 and 4. J. M. E. designed, performed, and analyzed experiments seen in Fig. 5 and assisted E. M. C. in the experiments shown in Fig. 4. All authors reviewed the results and approved the final version of the manuscript.

Acknowledgments—Data acquisition at the Macromolecular Diffraction (MacCHESS) facility at the Cornell High Energy Synchrotron Source (CHESS) was supported by the National Science Foundation Award DMR 0225180 and the National Institutes of Health Award RR-01646.

References

1. Varshavsky, A. (2012) The ubiquitin system, an immense realm. *Annu. Rev. Biochem.* **81,** 167–176
2. Pickart, C. M. (2001) Mechanisms underlying ubiquitination. *Annu. Rev. Biochem.* **70,** 503–533
3. Ciechanover, A., and Ben-Saadon, R. (2004) N-terminal ubiquitination: more protein substrates join in. *Trends Cell Biol.* **14,** 103–106
4. Scheffner, M., and Kumar, S. (2014) Mammalian HECT ubiquitin-protein ligases: biological and pathophysiological aspects. *Biochim. Biophys. Acta* **1843,** 61–74
5. Callaghan, M. J., Russell, A. J., Woollatt, E., Sutherland, G. R., Sutherland, R. L., and Watts, C. K. (1998) Identification of a human HECT family protein with homology to the *Drosophila* tumor suppressor gene hyperplastic discs. *Oncogene* **17,** 3479–3491
6. Mansfield, E., Hersperger, E., Biggs, J., and Shearn, A. (1994) Genetic and molecular analysis of hyperplastic discs, a gene whose product is required for regulation of cell proliferation in *Drosophila melanogaster* imaginal discs and germ cells. *Dev. Biol.* **165,** 507–526

7. Cojocaru, M., Bouchard, A., Cloutier, P., Cooper, J. J., Varzavand, K., Price, D. H., and Coulombe, B. (2011) Transcription factor IIS cooperates with the E3 ligase UBR5 to ubiquitinate the CDK9 subunit of the positive transcription elongation factor B. *J. Biol. Chem.* **286,** 5012–5022
8. Hay-Koren, A., Caspi, M., Zilberberg, A., and Rosin-Arbesfeld, R. (2011) The EDD E3 ubiquitin ligase ubiquitinates and up-regulates β-catenin. *Mol. Biol. Cell* **22,** 399–411
9. Honda, Y., Tojo, M., Matsuzaki, K., Anan, T., Matsumoto, M., Ando, M., Saya, H., and Nakao, M. (2002) Cooperation of HECT-domain ubiquitin ligase hHYD and DNA topoisomerase II-binding protein for DNA damage response. *J. Biol. Chem.* **277,** 3599–3605
10. Jung, H. Y., Wang, X., Jun, S., and Park, J. I. (2013) Dyrk2-associated EDD-DDB1-VprBP E3 ligase inhibits telomerase by TERT degradation. *J. Biol. Chem.* **288,** 7252–7262
11. Otwinowski, Z., and Minor, W. (1997) Processing of x-ray diffraction data collected in oscillation mode. *Methods Enzymol.* **276,** 307–326
12. Rutz, S., Kayagaki, N., Phung, Q. T., Eidenschenk, C., Noubade, R., Wang, X., Lesch, J., Lu, R., Newton, K., Huang, O. W., Cochran, A. G., Vasser, M., Fauber, B. P., DeVoss, J., Webster, J., *et al.* (2015) Deubiquitinase DUBA is a post-translational brake on interleukin-17 production in T cells. *Nature* **518,** 417–421
13. Wang, X., Singh, S., Jung, H. Y., Yang, G., Jun, S., Sastry, K. J., and Park, J. I. (2013) HIV-1 Vpr protein inhibits telomerase activity via the EDD-DDB1-VPRBP E3 ligase complex. *J. Biol. Chem.* **288,** 15474–15480
14. Yoshida, M., Yoshida, K., Kozlov, G., Lim, N. S., De Crescenzo, G., Pang, Z., Berlanga, J. J., Kahvejian, A., Gehring, K., Wing, S. S., and Sonenberg, N. (2006) Poly(A) binding protein (PABP) homeostasis is mediated by the stability of its inhibitor, Paip2. *EMBO J.* **25,** 1934–1944
15. Zhang, T., Cronshaw, J., Kanu, N., Snijders, A. P., and Behrens, A. (2014) UBR5-mediated ubiquitination of ATMIN is required for ionizing radiation-induced ATM signaling and function. *Proc. Natl. Acad. Sci. U.S.A.* **111,** 12091–12096
16. Bradley, A., Zheng, H., Ziebarth, A., Sakati, W., Branham-O'Connor, M., Blumer, J. B., Liu, Y., Kistner-Griffin, E., Rodriguez-Aguayo, C., Lopez-Berestein, G., Sood, A. K., Landen, C. N., Jr., and Eblen, S. T. (2014) EDD enhances cell survival and cisplatin resistance and is a therapeutic target for epithelial ovarian cancer. *Carcinogenesis* **35,** 1100–1109
17. Fuja, T. J., Lin, F., Osann, K. E., and Bryant, P. J. (2004) Somatic mutations and altered expression of the candidate tumor suppressors CSNK1ϵ, DLG1, and EDD/hHYD in mammary ductal carcinoma. *Cancer Res.* **64,** 942–951
18. Meissner, B., Kridel, R., Lim, R. S., Rogic, S., Tse, K., Scott, D. W., Moore, R., Mungall, A. J., Marra, M. A., Connors, J. M., Steidl, C., and Gascoyne, R. D. (2013) The E3 ubiquitin ligase UBR5 is recurrently mutated in mantle cell lymphoma. *Blood* **121,** 3161–3164
19. Ohshima, R., Ohta, T., Wu, W., Koike, A., Iwatani, T., Henderson, M., Watts, C. K., and Otsubo, T. (2007) Putative tumor suppressor EDD interacts with and up-regulates APC. *Genes Cells* **12,** 1339–1345
20. Henderson, M. J., Munoz, M. A., Saunders, D. N., Clancy, J. L., Russell, A. J., Williams, B., Pappin, D., Khanna, K. K., Jackson, S. P., Sutherland, R. L., and Watts, C. K. (2006) EDD mediates DNA damage-induced activation of CHK2. *J. Biol. Chem.* **281,** 39990–40000
21. Ling, S., and Lin, W. C. (2011) EDD inhibits ATM-mediated phosphorylation of p53. *J. Biol. Chem.* **286,** 14972–14982
22. Smits, V. A. (2012) EDD induces cell cycle arrest by increasing p53 levels. *Cell Cycle* **11,** 715–720
23. Su, H., Meng, S., Lu, Y., Trombly, M. I., Chen, J., Lin, C., Turk, A., and Wang, X. (2011) Mammalian hyperplastic discs homolog EDD regulates miRNA-mediated gene silencing. *Mol. Cell* **43,** 97–109
24. Kozlov, G., Nguyen, L., Lin, T., De Crescenzo, G., Park, M., and Gehring, K. (2007) Structural basis of ubiquitin recognition by the ubiquitin-associated (UBA) domain of the ubiquitin ligase EDD. *J. Biol. Chem.* **282,** 35787–35795
25. Kozlov, G., Trempe, J. F., Khaleghpour, K., Kahvejian, A., Ekiel, I., and Gehring, K. (2001) Structure and function of the C-terminal PABC domain of human poly(A)-binding protein. *Proc. Natl. Acad. Sci. U.S.A.* **98,** 4409–4413
26. Matta-Camacho, E., Kozlov, G., Menade, M., and Gehring, K. (2012) Structure of the HECT C-lobe of the UBR5 E3 ubiquitin ligase. *Acta Crystallogr. Sect. F Struct. Biol. Cryst. Commun.* **68,** 1158–1163
27. Deo, R. C., Sonenberg, N., and Burley, S. K. (2001) X-ray structure of the human hyperplastic discs protein: an ortholog of the C-terminal domain of poly(A)-binding protein. *Proc. Natl. Acad. Sci. U.S.A.* **98,** 4414–4419
28. Xie, J., Kozlov, G., and Gehring, K. (2014) The "tale" of poly(A) binding protein: the MLLE domain and PAM2-containing proteins. *Biochim. Biophys. Acta* **1839,** 1062–1068
29. Albrecht, M., and Lengauer, T. (2004) Survey on the PABC recognition motif PAM2. *Biochem. Biophys. Res. Commun.* **316,** 129–138
30. Kozlov, G., De Crescenzo, G., Lim, N. S., Siddiqui, N., Fantus, D., Kahvejian, A., Trempe, J. F., Elias, D., Ekiel, I., Sonenberg, N., O'Connor-McCourt, M., and Gehring, K. (2004) Structural basis of ligand recognition by PABC, a highly specific peptide-binding domain found in poly(A)-binding protein and a HECT ubiquitin ligase. *EMBO J.* **23,** 272–281
31. Kozlov, G., Ménade, M., Rosenauer, A., Nguyen, L., and Gehring, K. (2010) Molecular determinants of PAM2 recognition by the MLLE domain of poly(A)-binding protein. *J. Mol. Biol.* **397,** 397–407
32. Lim, N. S., Kozlov, G., Chang, T. C., Groover, O., Siddiqui, N., Volpon, L., De Crescenzo, G., Shyu, A. B., and Gehring, K. (2006) Comparative peptide binding studies of the PABC domains from the ubiquitin-protein isopeptide ligase HYD and poly(A)-binding protein. Implications for HYD function. *J. Biol. Chem.* **281,** 14376–14382
33. Kozlov, G., Safaee, N., Rosenauer, A., and Gehring, K. (2010) Structural basis of binding of P-body-associated proteins GW182 and ataxin-2 by the Mlle domain of poly(A)-binding protein. *J. Biol. Chem.* **285,** 13599–13606
34. Jinek, M., Fabian, M. R., Coyle, S. M., Sonenberg, N., and Doudna, J. A. (2010) Structural insights into the human GW182-PABC interaction in microRNA-mediated deadenylation. *Nat. Struct. Mol. Biol.* **17,** 238–240
35. McCoy, A. J., Grosse-Kunstleve, R. W., Adams, P. D., Winn, M. D., Storoni, L. C., and Read, R. J. (2007) Phaser crystallographic software. *J. Appl. Crystallogr.* **40,** 658–674
36. McRee, D. E. (1999) XtalView/Xfit–a versatile program for manipulating atomic coordinates and electron density. *J. Struct. Biol.* **125,** 156–165
37. Murshudov, G. N., Vagin, A. A., Lebedev, A., Wilson, K. S., and Dodson, E. J. (1999) Efficient anisotropic refinement of macromolecular structures using FFT. *Acta Crystallogr. D Biol. Crystallogr.* **55,** 247–255
38. Winn, M. D., Murshudov, G. N., and Papiz, M. Z. (2003) Macromolecular TLS refinement in REFMAC at moderate resolutions. *Methods Enzymol.* **374,** 300–321
39. Laskowski, R. A., MacArthur, M. W., Moss, D. S., and Thornton, J. M. (1993) PROCHECK: a program to check the stereochemical quality of protein structures. *J. Appl. Crystallogr.* **26,** 283–291
40. Vriend, G. (1990) WHAT IF: a molecular modeling and drug design program. *J. Mol. Graph.* **8,** 52–56
41. Delaglio, F., Grzesiek, S., Vuister, G. W., Zhu, G., Pfeifer, J., and Bax, A. (1995) NMRPipe: a multidimensional spectral processing system based on UNIX pipes. *J Biomol. NMR* **6,** 277–293
42. Bartels, C., Xia, T. H., Billeter, M., Güntert, P., and Wüthrich, K. (1995) The program XEASY for computer-supported NMR spectral analysis of biological macromolecules. *J. Biomol. NMR* **6,** 1–10
43. Gallagher, E., Gao, M., Liu, Y. C., and Karin, M. (2006) Activation of the E3 ubiquitin ligase Itch through a phosphorylation-induced conformational change. *Proc. Natl. Acad. Sci. U.S.A.* **103,** 1717–1722
44. Mari, S., Ruetalo, N., Maspero, E., Stoffregen, M. C., Pasqualato, S., Polo, S., and Wiesner, S. (2014) Structural and functional framework for the autoinhibition of Nedd4-family ubiquitin ligases. *Structure* **22,** 1639–1649
45. Wiesner, S., Ogunjimi, A. A., Wang, H. R., Rotin, D., Sicheri, F., Wrana, J. L., and Forman-Kay, J. D. (2007) Autoinhibition of the HECT-type ubiquitin ligase Smurf2 through its C2 domain. *Cell* **130,** 651–662
46. Ichimura, T., Yamamura, H., Sasamoto, K., Tominaga, Y., Taoka, M., Kakiuchi, K., Shinkawa, T., Takahashi, N., Shimada, S., and Isobe, T. (2005) 14-3-3 proteins modulate the expression of epithelial Na^+ channels by phosphorylation-dependent interaction with Nedd4-2 ubiquitin ligase. *J. Biol. Chem.* **280,** 13187–13194
47. Shea, F. F., Rowell, J. L., Li, Y., Chang, T. H., and Alvarez, C. E. (2012) Mammalian α-arrestins link activated seven transmembrane receptors to

Nedd4 family E3 ubiquitin ligases and interact with β-arrestins. *PLoS ONE* **7,** e50557
48. Shearwin-Whyatt, L., Dalton, H. E., Foot, N., and Kumar, S. (2006) Regulation of functional diversity within the Nedd4 family by accessory and adaptor proteins. *Bioessays* **28,** 617–628
49. Pandya, R. K., Partridge, J. R., Love, K. R., Schwartz, T. U., and Ploegh, H. L. (2010) A structural element within the HUWE1 HECT domain modulates self-ubiquitination and substrate ubiquitination activities. *J. Biol. Chem.* **285,** 5664–5673
50. Bethard, J. R., Zheng, H., Roberts, L., and Eblen, S. T. (2011) Identification of phosphorylation sites on the E3 ubiquitin ligase UBR5/EDD. *J. Proteomics* **75,** 603–609